

## BRAZILIAN HIGH TEMPERATURE PROCESSED STEELS FOR PIPELINES

Ivani de S. Bott  
Associate Professor, DCMM/PUC-Rio. Rua Marquês de São Vicente 225, Rio de Janeiro-RJ,  
22453-900 Brasil,  
[bott@dcomm.puc-rio.br](mailto:bott@dcomm.puc-rio.br)

Gilmar Zacca Batista  
MsC, Pipeline Engineer  
Engineering Petrobras /IETEG/ETEG/EDUT  
[gzacca@petrobras.br](mailto:gzacca@petrobras.br)

Eduardo Hippert, Jr  
Dr., Senior Engineer  
PETROBRAS/CENPES/TMEC  
[hippert@petrobras.br](mailto:hippert@petrobras.br)

Luís F. G. de Souza  
Adjunct Professor, DEPMC/CEFET-RJ. Av. Maracanã, 229 Bl. E-516, Rio de Janeiro-RJ,  
20271-110 Brasil,  
[lfelipe@cefet-rj.br](mailto:lfelipe@cefet-rj.br)

Paulo R. Rios  
Professor, UFF/EEIMVR, Av. dos Trabalhadores, 420, Volta Redonda, RJ,  
27255-125 BRASIL  
[prrios@metal.eeimvr.uff.br](mailto:prrios@metal.eeimvr.uff.br)

Keywords: steels, mechanical properties, microstructure, welding, stress corrosion, pipelines

### Abstract

The present work continues part of an extensive program developed at PUC-Rio initiated in 2000 in collaboration with industry and other Brazilian research institutes, to facilitate the application of API 5L X80 linepipe in Brazilian construction projects.

The production of API class steels using the traditional controlled rolling route, rather than accelerated cooling, as used in many other countries, necessitates a careful adjustment of steel composition combined with the optimisation of the rolling schedule for the deformation and phase transformation characteristics of these modified alloys.

In the first part of this study, the evaluation of two Nb-Cr and NbCrMo steels systems was undertaken at two stages in the production route, this involved sampling the material as plate and as the final tubular product. Mechanical and microstructural characterization of the plate and tube, including the longitudinal (SAW) and circumferential SMAW weld were undertaken, as well as laboratory investigations of Environmentally Induced Cracking. The second part of this study evaluated the effect of the induction bending process on the microstructure and mechanical properties of the pipe obtained from a NbCrMoV steel system

## Introduction

The significant economic advantages of transporting crude oil and gas by pipeline has led not only to a growing demand for extensive pipeline networks, but also to a need to increase the capacity of the existing ones. Such an increase in capacity necessitates the installation of larger diameter pipes with higher operating pressures, and consequently requires the use of thicker walled pipes and/or higher strength steels.

Increasing the strength of the pipeline material, can permit a significant reduction in wall thickness thereby resulting in economic benefits due to the reduction in overall weight. Such savings are especially important for pipeline construction in remote locations, where any weight reduction can be critical in reducing basic costs such as those associated with transport, and manipulation during construction and welding.

The cost of pipes represents approximately 50 percent of total pipeline construction costs. The use of new grades with yield strength as high as X80 results in savings of between 10 and 15 percent in the pipe costs, including reduction of costs related to pipe transport, because the pipes have lower weight, as well as a reduction in the welding costs in terms of lower overall weld mass and fewer hours/welder.

A particularly important advance in the development of pipeline steels occurred in the 1970's with the introduction of thermomechanical processing to substitute for the traditional normalizing heat treatment production routes. This became the basis for the manufacture of X-70 steels which soon represented the industry standard for pipeline construction [1].

The subsequent introduction of accelerated cooling, after controlled rolling, led to the possibility of producing steels with even higher strength levels. The API-X80 steels, though up to now relatively little used in Brazil, have been very successfully exploited worldwide in pipeline construction. These steels have been manufactured using a production route, which includes accelerated cooling at cooling rates of 15 to 20°C /s until reaching a temperature of around 550°C, after which air cooling is used. It should be mentioned that the steels of this study, for pipeline applications, were produced without accelerated cooling.

Gas production and consumption in Brazil are growing more and more. According to Petrobras' Strategic Plan, the growth perspective of the natural gas market is from 30,7 million m<sup>3</sup>/day in 2003 to 77,6 million m<sup>3</sup>/day in 2010 [2]. To meet this demand, the new gas pipelines must have larger diameters and operate with higher pressures, resulting in the need for a pipe wall thickness increase or higher strength steels. Increasing the strength of the steel with the same diameter and pressure reduces the need for very high wall thicknesses. The main objectives are to make possible high pressure projects and economy steel, thereby reducing the weight and, therefore, the costs on pipe purchases and pipeline construction.

As mentioned previously, in Brazil, the trial production of high strength API 5L Grade X-80 specification, is made with the traditional controlled rolling process, ie. differently from the accelerated cooling process that is used in other countries. Although successfully developed in Brazil, as shown in it first part of this study [3], X80 pipe has not been used in either offshore or onshore pipelines. For this reason, it is necessary to evaluate the pipe behaviour under field construction conditions, more specifically in the bending and welding processes.

Also, there is urgency in optimising and extending the resources for corrosion control to minimise problems regarding failure and leakage in these pipelines. Corrosion control is especially important, as it is clearly associated with mechanical integrity. This has led to an effort to produce alloys with better mechanical properties, which consequently will gradually

permit a reduction in the thickness of the pipeline walls. However it is necessary to bear in mind that internal corrosion occurs and it can compromise the use of these materials. This is so because as long as the wall thickness is diminished, the corrosion can lead to catastrophic failures and reduce tube lifetimes significantly. Therefore, it is necessary to study the behaviour of the steel in critical environments to understand this behaviour and to obtain better performance, and moreover, to predict the relevant corrosion rates.

In pipeline construction, depending on the field profile, about 30% to 40% of the pipes are bent. The preference is for cold bending, because this can be performed on site. However, when the bend radius is small, it becomes necessary apply a hot bending process. This process causes a located heating and fast cooling of the pipe section that undergoes bending, which can cause significant microstructural changes in the steel and, consequently, changes in the mechanical properties.

### Materials

Table I shows the chemical compositions of the four groups of microalloyed steels, three of X80 and one of X70 grade, which were studied. The X80, NbCr and NbCrMo steels were, supplied in the form of 16 mm plates (samples A to L) and also as tubes of 30” of diameter A, D, G, and J, produced by the UOE process. In the UOE fabrication process, the plate is cold pressed into “U” and to “O” formats sequentially, followed by internal and external welding by the submerged arc process. After this welding stage, the pipe is “expanded” (E). The X80 steel NbCrMoV, were supplied in the form of tube 50,8 mm (20 in) in diameter and 19mm in thickness. This table also shows the chemical composition of the weld metal (WM) for the longitudinal weld of the different systems of X80 and of the X70 grades, and the composition of the circumferential weld for the NbCrMo system.

Table 1 - Chemical composition of the four groups of microalloyed steels.

Sample	Plate/Pipe	Elements (mass %)								
		C	Mn	Si	Nb	V	Ti	Cr	Mo	N
NbCrMo (X80)	A	0.07	1.76	0.18	0.071	_____	0.014	0.20	0.16	0.006
	D	0.04	1.75	0.17	0.073	_____	0.013	0.21	0.16	0.004
NbCr (X80)	G	0.04	1.85	0.18	0.073	_____	0.016	0.32	0.03	0.004
	J	0.04	1.86	0.19	0.075	_____	0.017	0.33	0.03	0.005
X70	_____	0.06	1.55	0.18	0.055	_____	0.017	0.02	_____	0.0071
NbCrMoV (X80)	_____	0.05	1.76	0.17	0.066	0.025	0.016	0.15	0.20	0.0057
WM (SAW)	X70	0.06	1.57	0.34	0.026	0.046	0.010	0.06	0.199	_____
WM (SAW)	NbCr/NbCrMo	0.75	1.92	1.92	0.044	_____	0.013	0.16	0.291	_____
WM (SMAW)	NbCrMo	0.07	1.21	0.35	0.019	_____	0.03	0.04	0.01	_____
WM (SAW)	NbCrMoV	0.06	1.54	0.32	0.037	0.015	0.013	0.102	0.205	_____

## Methodology

### Mechanical properties

In the present study, the microstructure obtained is correlated with both the resulting mechanical properties, the weldability and strength, exhibited by the materials in aggressive environments. According to the API 5L 2000 specification [4] standard tensile testing, Charpy impact testing and hardness measurements were utilized to determine mechanical properties and microstructural characterization was performed exploiting optical and scanning electron microscopy. This study also evaluated the influence of the hot bending process and heat treatment on the microstructure and mechanical properties of the NbCrMoV Steel.

### Weldability

With regard to weldability, the two NbCr/NbCrMo steels were studied, including both longitudinal and circumferential welds, the latter being evaluated according to the API-1104 [5] standard.

In the present study three types of electrodes were used. The chemical compositions and typical mechanical properties, as informed by the manufacturer, are detailed in Tables II and III. All electrodes were stored under vacuum, in sealed packets prior to use. The welding pass sequence included the use of E-6010 electrodes for the root pass, and E-9010G for the second and third passes. Basic E-10018G electrodes were used for the filler and finishing passes. The circumferential weld was performed in tube A, the chemical composition of which is shown in the Table I. The welded joint was evaluated according to the API-1104 [5] specification.

Table II – Typical chemical composition of the weld metal.

Electrode	Chemical Composition (wt.%)							
	C	Mn	Si	P	S	Ni	Mo	Cu
E-6010	0.14	0.56	0.18	-	0.012	-	-	-
E-9010-G	0.12	0.62	0.12	0.013	0.014	0.67	0.02	0.03
E-10018-G	0.085	1.26	0.42	0.009	0.006	2.07	-	-

Table III – Mechanical Properties of the weld metal.

Electrode	Charpy-V (J) -20 °C	YS (MPa)	UTS (MPa)	EL (%)
E-6010	95	450	520	26
E-9010-G	75	610	650	21
E-10018-G	120	670	730	24

### Welding Procedure

Full-scale girth welding was undertaken in the laboratory using field techniques involving two welders. 762mm (30 in) diameter pipes of 16mm wall thickness were circumferentially welded using coated electrodes. The welding parameters utilized, and electrode specifications are detailed in Table IV.

Table IV – Welding parameters and electrode for each type of pass.

Pass	Electrode	Type / Polarity	Voltage (V)	Current (A)	Heat Input (kJ/mm)
Root “Hot”	E-6010 Ø 4 mm	CC (-)	27	130	0.9
	E-9010G Ø 4 mm	CC (+)	27	135	0.9
Filling	E-10018G Ø 4.5 mm	CC (+)	25	200	1.2
Finishing	E-10018G Ø 4.5 mm	CC (+)	25	195	1.2
Preheat Temperature = 150 °C; Inter-pass Temperature = 250 °C					

The average yield stress (YS) of the welded joint under investigation was 690MPa, and that of the pipe itself, 695MPa. The API 5L technical specification indicates a range of 621-827 MPa for such pipeline material. It is believed that electrodes with cellulose-based coatings may be of limited use since it is difficult to obtain sufficiently high strength levels, without compromising toughness levels and the resistance to hydrogen induced cracking.

The mechanical tests undertaken to qualify the welding procedure were carried out according to API-1104 [5], which requires tensile, bending and nick-break tests on material from all four quadrants of the welded joint.

### Corrosion behaviour

In order to perform the evaluation of the behaviour of the Nb-Cr steels in an aggressive environment, and more specifically the resistance to the deleterious effects of H<sub>2</sub>S, slow strain rate (SSR) tests were carried out, which involved immersing the samples in a solution of sodium thiosulphate. Constant load tests were also conducted according to the standard NACE TM0177/96 METHOD A [6].

The objective was to evaluate the SCC and hydrogen embrittlement (HE) behaviour of API-X70 and API-X80 class pipeline steel G, Table I, using SSRT and NACE 0177/96 - Method A testing. [7] The solutions used for both tests are detailed in Table V.

Table V – Chemical composition of the solutions for SSRT and NACE tests.

Composition of the Test Solutions		
Component	SSRT test	NACE test
	Content	
Sodium Thiosulphate (Na <sub>2</sub> S <sub>2</sub> O <sub>3</sub> )	10 <sup>-3</sup> mol/l	-----
Sodium Chloride (NaCl)	5%vol	5%vol
Acetic Acid (CH <sub>3</sub> COOH)	0.5%vol	-----
Glacial Acetic Acid (CH <sub>3</sub> COOH)	-----	0.23%vol
Sodium Acetate (CH <sub>3</sub> COONa)	-----	0.4%vol

After the test, the surfaces of the test pieces, which had been exposed to the NACE solution, were cleaned in accordance with the ASTM G-1-95 standard, thereby permitting metallographic examination to determine whether or not surface cracks had been produced [8].

The 50.8x 19 mm (20 x 0.75 in) API 5L X80 pipe, of the NbCrMoV system produced by the UOE process, was used for this study. Table I shows the steel chemical composition [9].

### Hot bending process

The hot bending process, involved the pipe end being pushed while a rotating arm, which guides the pipe during the bending to achieve the desired bend radius, fixes the other end.

During bending, the pipe passes through a high frequency coil that creates a concentrated magnetic field and induces an electric potential in the pipe creating a current flow. The pipe resistance to the current flow causes fast and localised heating that is followed by water quenching applied at the external pipe surface. The bending temperature was around 1050°C and a 2.54 m bend radius was produced, resulting in a 70° bend angle. Figure 1 illustrates the process.



Figure 1 - The 20in. X80 bending process. Notice that, just after the heating coil, the pipe is water cooled.

To evaluate the effect of bending on the pipe, mechanical tests (tensile, Charpy V-notch and micro hardness) and dimensional analysis was undertaken. The mechanical tests were carried out according to API 5L [10] and ASTM A 370 [11] standards. Tensile properties were measured using transverse round bar specimens. Impact properties were measured using transverse, full size Charpy V-notch specimens where the long dimension was parallel to the circumferential direction. In addition, a microstructural analysis was performed. The locations for the extraction of samples are shown in Figure 2.

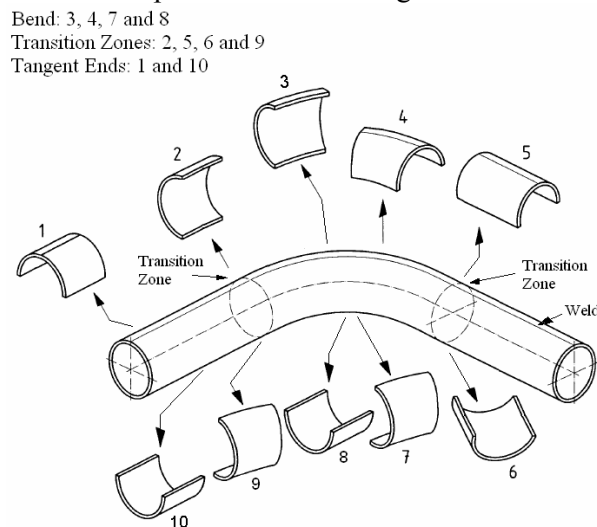


Figure 2 - Location for extraction of samples for testing.

## Results and Discussion

### Formability

The mechanical properties of the steels at the plate stage of production are different from those in the final tubular product. In considering the tensile strength aspects of the plate steel, one must take this aspect into account as it can affect the subsequent deformation from plate

to tubular product since the UOE process involves cold working at this stage of the manufacturing routine. This cold working during the bending of the plate and expanding the tube will impose at least one stress reversal on the material. The Nb-Cr and NbCrMo [3] steels in this study exhibited a ferritic microstructure, which contains the MA microconstituent, and which on straining can effectively impede dislocation movement. MA dislocation barriers cause dislocation pileups and consequent back stresses, which impede further dislocation motion in the region. When such a steel is subjected to deformation in the opposite direction to that originally applied (“reverse deformation”) the back stresses resulting from the previously formed dislocation pileups facilitate the new deformation, effectively softening the material [12] (Bauschinger Effect). An increase in strength after pipe forming was obtained for the Nb-Cr and NbCrMo steels, as shown in Figure 3, and the resulting yield stress: UTS ratio was below 0.93, the maximum permitted by the API 5L standard [4].

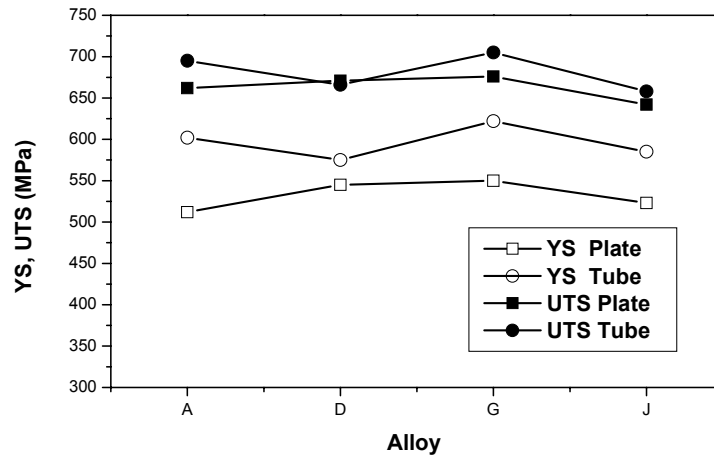


Figure 3- Relationship between YS and UTS for the plates and tubes A, D, G and J, of the system Nb-Cr and NbCrMo.

### Weldability

It is known that the thermal cycles associated with the industrial welding process used in pipeline fabrication and construction can lead to localized increases in hardness in the HAZ [13] and possibly a reduction in yield strength. No such increase was observed however, for the steels and conditions studied in the current work, where the average hardness for the plate and tube was of approximately 240 HV<sub>100gf</sub> while the HAZ was approximately 220 HV<sub>100gf</sub>. A similar result was presented by Sarma [14] for a quenched and tempered HSLA100 steel of 14mm thickness, with composition of 0.04%C, 0.87%Mn, 0.25%Si, 0.5%Cr, 3.54%Ni, 0.57Mo%, 0.038%Nb, after welding at a heat input of 2kJ/mm. It should be noted that the heat input applied in this study was approximately 40J/cm and the reduction in hardness observed for the HAZ did not significantly affect the tensile performance of the steel, as compared with the plate and the welded joint, as shown in Figure 4. It was also observed that, in all cases, the location of rupture during tensile testing of the welded joints, was in the base metal, away from the heat affected zone.

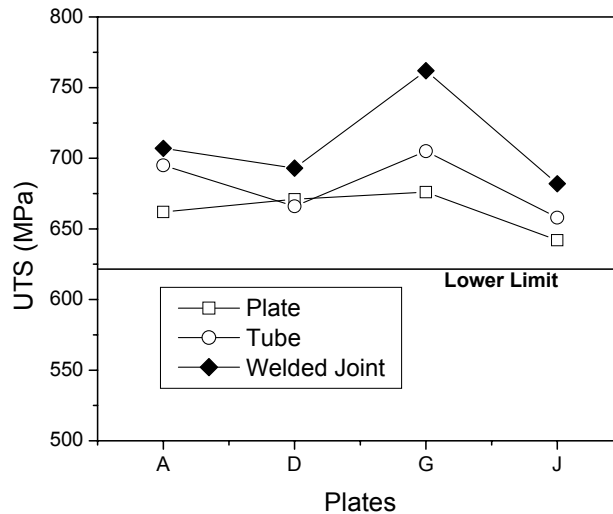


Figure 4- UTS values for the plates, tubes and their HAZ for the Nb-Cr and NbCrMo steels.

Nagae [15] obtained excellent yield strengths for a steel containing 0.06%C, 0.15%Mo, 0.04%Nb, 0.04%V (corresponding to a Pcm of 0.18%) despite some softening of the HAZ. This composition is similar to that of steel A in the current study. Nagae [15] utilizes the concept of relative thickness in his study, considering the maximum extent of the softened region within the HAZ divided by the wall thickness of the tube. This author proposed that when this relative thickness is less than 0.2, the softening of the HAZ would have no significant effect on the overall yield stress of the welded joint. It is suggested, furthermore, that the presence of Nb and V (as in the steels considered in the current work) effectively reduce this relative thickness.

A low susceptibility to cold cracking for given steel with low oxygen and sulphur contents may be predicted purely on the basis of the calculated CE value. This may not always serve as a good prediction of the steel's real behaviour since, in practice, other factors will exert additional influence. The susceptibility can often be more pronounced than would be indicated by the CE approach, in cases where the absence of non-metallic inclusions leads to a reduction in the nucleation rate of polygonal Ferrite [16]. When present, these inclusions can, indirectly, promote a lower susceptibility to cold cracking by raising the ferrite nucleation rate. Such an improvement can, under service conditions, even permit the elimination of pre-heating routines and/or promote an increased tolerance for hydrogen contamination when using coated electrodes [17]. The average Pcm value for the steels in this study was 0.16%, which is lower than the 0.25% upper limit specified in the API 5L standard, thus indicating good weldability.

Overall, the increase in HAZ hardness, in some cases associated with the presence of MA, is accompanied by a reduction in yield strength and UTS [16,18]. Thompson and Krauss [18], however, comment that the yield strength is expected to be higher for a low carbon bainitic microstructure which does contain MA, than for a bainitic microstructure composed of ferrite laths or acicular Ferrite of high dislocation density and with little or no carbide precipitation (without MA). The microstructure obtained in the WM and HAZ for welds performed under industrial production conditions for the steels under study exhibited MA. The volume fraction was determined for the three regions of the welded joint, base metal (plate), HAZ and the weld metal. The volume fraction was highest in the weld metal.

The presence of the MA microconstituent is generally considered to provoke low toughness [20,21,22] both for the HAZ and the WM [18]. The effect of the MA on the toughness of the

base metal, HAZ and WM is shown in Figure 5, where the temperatures associated with the 100J absorbed impact energy in the Charpy curves for these steels, clearly indicate that the HAZ exhibits a higher toughness than the tube base metal.

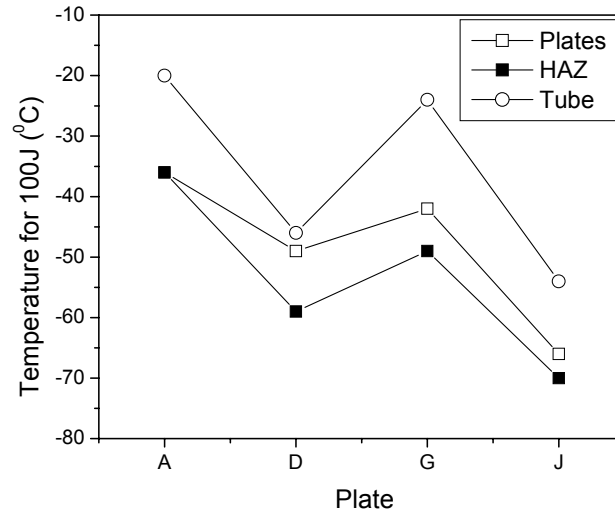


Figure 5- Toughness values for the plates, tubes and HAZ, for the system Nb-Cr and NbCrMo, considering the energy of 100.

### Girth welding

The traditional circumferential welding process for pipelines involves the use of electrodes with cellulose-based coatings, due to their versatility. With the adoption of higher strength steels, toughness constraints and the relatively high levels of residual hydrogen in the weld metal (which can reach levels of up to 50ml/100g) may subsequently lead to cracking in the heat affected zone (HAZ), therefore the use of such electrodes becomes less attractive.

It has been suggested [24,25] that optimum results can be achieved utilizing a combination of electrode types. The cellulosic electrodes offer good penetration and are therefore preferred for the root pass. Lower strength filler metal is acceptable in this region since the subsequent hot pass with a filler metal of higher strength also effectively tempers the root pass material and its HAZ. Additionally, the lower strength of the root pass renders this material more able to absorb the stresses generated during the deposition of the following passes, thereby helping to avoid crack formation due to the concentration of high residual stress levels at the root of the joint. It should be remembered that, in practice, some dilution of the filler metal by subsequent passes also occurs, thereby causing some strengthening of the originally deposited material [26].

For the filling and finishing passes, high strength basic electrodes are suggested [25] utilizing a vertical down position. Though the welding speed itself is slower than that attainable using cellulose coated electrodes, joint filling is quicker due to the high deposition rate, thereby permitting completion of the joint with a reduced number of passes.

The average yield stress obtained from the tensile test results for the welded joint was 690MPa as shown in Table VI. The lowest acceptable YS level for this class of steel, according to the API 5L [4] specification is 621MPa. The tensile test pieces were observed to exhibit ductile fracture (Figure 6a), and rupture was found to occur outside the weld metal and HAZ for all four quadrants.

Table VI – Tensile test results for the welded joint for the UR=upper right, UL=upper left, LR=lower right, LL=lower left.

Quadrant	Test piece dimensions (mm)	Cross sectional area (mm <sup>2</sup> )	YS (MPa)	Rupture location
UR	25.39 x 15.81	401.42	690	Base metal
LR	25.30 x 15.77	398.98	685	Base metal
UL	25.40 x 15.90	406.86	690	Base metal
LL	25.35 x 15.72	398.50	695	Base metal

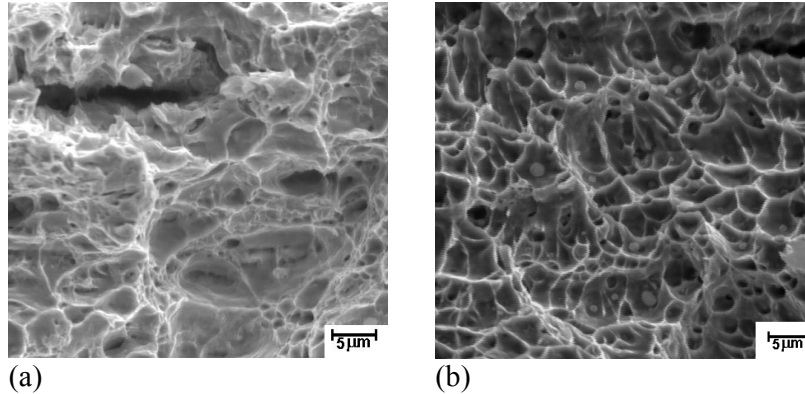
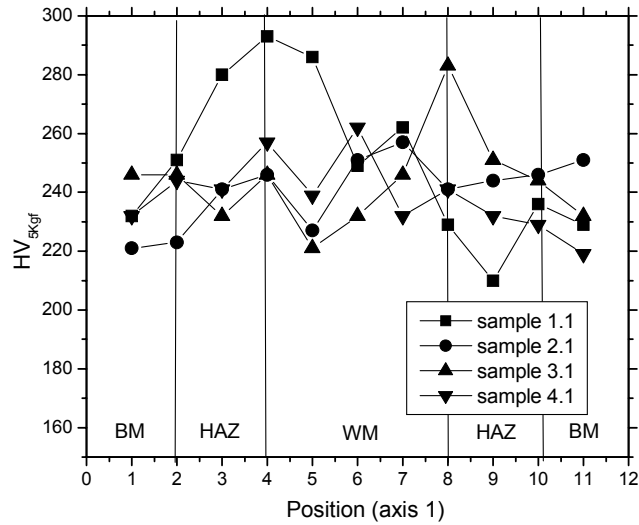


Figure 6 – Scanning electron micrographs of fracture surfaces (showing ductile nature of fractures) (a) Tensile test; (b) “Nick-break” test.

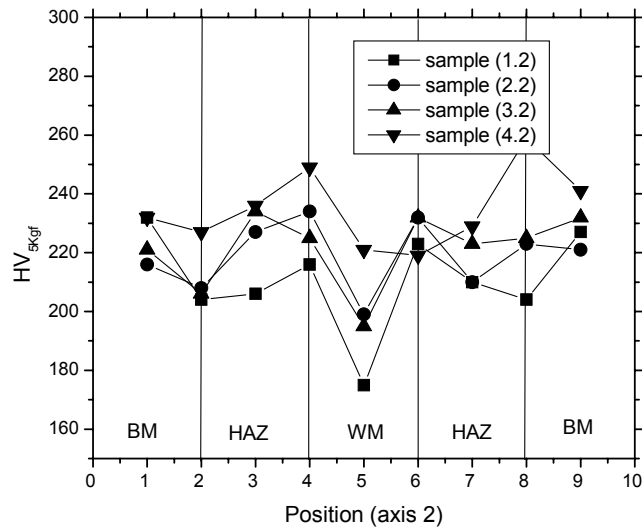
The heating applied during welding and the subsequent rate of cooling can adversely affect the HAZ. In particular, the excellent combination of strength and toughness of the Ferrite-Bainite, control-rolled HSLA steels investigated in this study can be degraded and local brittle zones may arise. In order to evaluate modifications resulting from the thermal cycling, mapping of (5kgf) Vickers hardness levels across the welded joint was carried out. Figure 7a and 7b show a schematic diagram of the results obtained at 0.5mm from the upper and lower surfaces of the welded joint, which corresponds to the position of the axis 1 and axis 2, which are associated with the hardness of the different regions sampled.

It can be observed that the HAZ, except in the case of one of the samples, exhibited hardness values similar to the BM and the strongest region of the WM also exhibited hardness levels similar to those of the BM. The lower strength root pass exhibited correspondingly lower hardness levels as expected.

It should be observed that the average hardness of the HAZ of plate A, for the circumferential weld, was lower than that of the longitudinal weld (Table VII), indicating that this alloy did not show any tendency to harden, therefore exhibited a low probability to have cold cracks for the conditions studied. The gradient promoted by the heat input of the circumferential weld and the subsequent cooling rate was not sufficient to induce cold cracking in the HAZ.



(a) Hardness profile of the axis I



(b) Hardness profile of the axis II

Figure 7 – Hardness profiles along axis I(a) and II(b).

Table VII- Hardness values for steel A.

Hardness for Steel A from the NbCrMo System	
Condition	Hardness, Hv5
Plate	245
Tube	223
Longitudinal HAZ	242
Circumferential HAZ	230

Figure 8 presents the results of the Charpy V-notch impact tests, undertaken to evaluate the toughness of the weld metal. The material for the test pieces was extracted from regions 5mm below the surface (both upper and lower) in order to analyse both the root pass and the

finishing pass. Comparison of these results, with those for the BM (test piece notch aligned with the longitudinal direction of the pipe), showed that that the WM and BM exhibited similar toughness levels.

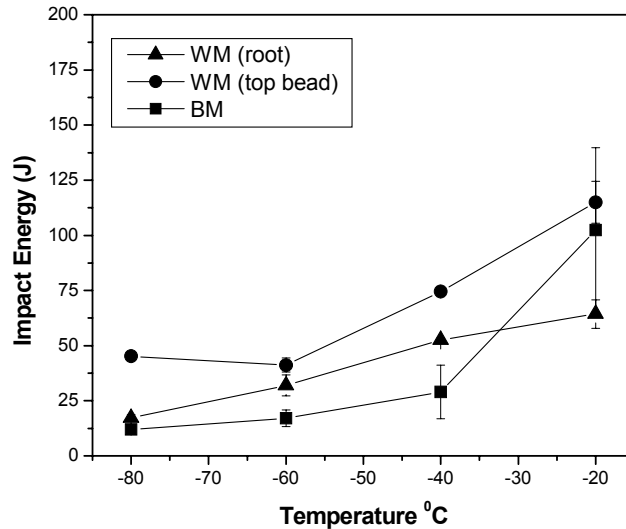


Figure 8 – Charpy V-notch impact test results, comparing toughness values for the root pass, the finishing pass and the base metal.

The results presented permit the following conclusions, The welding procedure used in the study, involving the utilization of several electrode types with a range of mechanical properties produced a joint which was adequate to attend the specifications of the API 1104 standard, and despite the high strength of the (Ferrite + Bainite + MA) base metal, no significant loss in toughness was identified for the heat affected zone, and the preheating and interpass temperatures used permitted the avoidance of cold cracking. The welding parameters used resulted in microstructures throughout the joint, which exhibited satisfactory toughness levels.

### **Integrity in Aggressive Environments**

#### **Resistance to SCC (SSRT and NACE test )**

##### **Body Pipe**

Oilfield service conditions involving high-pressure oil and gas with high CO<sub>2</sub>, H<sub>2</sub>S and chloride contents demand pipeline steels not only of high mechanical strength, but also high resistance to corrosion and to hydrogen embrittlement (HE) phenomena. The nucleation and growth of cracks in pipelines constructed of plain carbon and low alloy steels, when exposed to fluids containing H<sub>2</sub>S, have resulted in catastrophic failures. Furthermore, in practice, adequate formability and good weldability are, of course, also critical factors. Theoretically, three basic conditions must be fulfilled for SCC to occur; a corrosive medium, a tensile load and the inherent susceptibility of the steel in question [27,28,29].

The slow strain rate test has been widely exploited as a laboratory technique to evaluate the susceptibility of metallic materials to SCC and HE. In the case of candidate steels for service in the petrochemical industry, the SSRT is of particular interest since the relative speed of the high-load test permits suitably wide-ranging appraisals, involving the generation of a

significant number of results in a relatively short period. By contrast, the NACE 0177-96 - Method [6] is used to evaluate SCC resistance according to a fracture/no fracture criterion, and the degree to which internal cracks are developed in test pieces subjected to constant uniaxial elastic strain in the standard NACE solution, at ambient temperature and pressure.

The API-X70 steel exhibited a ferrite-pearlite microstructure, whereas the API-X80 grade had a microstructure composed of granular bainite with 3.4vol% of MA constituent . The API-X70 steel exhibited ductile characteristics when SSRT tested in air. This ductile behaviour changed to cleavage when the steel was tested in thiosulphate based solution, indicating some degree of embrittlement, where few plastically deformed regions were found. These observations are sustained by the fact that the fracture section was elliptical, the mode of fracture was ductile and accompanied by a reduction in cross sectional area of 68% during the test in air while this reduction is 17% when testing in thiosulphate-based solution.

The same tests were repeated for the API-X80 steel. For the SSRT in air, the fracture was characteristically ductile, with dimples on the fracture surface and regions of extensive plastic deformation being evident. In the thiosulphate-based solution, this steel also exhibited brittle fracture characteristics. The overall reduction in cross sectional area at fracture was 60% when tested in air and when tested in the thiosulphate-based solution, the reduction in area was reduced to just 7 percent. These results indicate some susceptibility to embrittlement.

Analysis of the longitudinal sections of the API-X70 and API-X80 test pieces, after thiosulphate solution testing, did not reveal secondary internal or surface cracks for either steel. The final fracture was associated with plastic collapse as a consequence of the small remaining area. The relationship between  $\sigma_f$  (fracture strength) and time to fracture (Figure 9) shows that the time to fracture was longer when tested in the air than in the thiosulphate-based solution, and this time was longer for the API-X80 than for the API-X70.

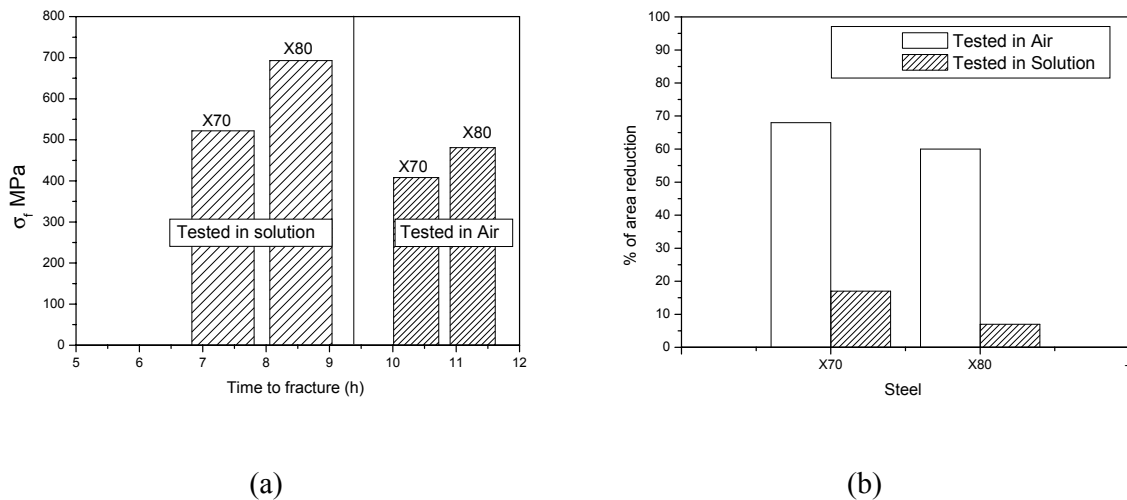


Figure 9- Behaviour of API-X70 and API-X80 when tested in air and in thiosulphate solution, (a) Time to fracture and (b) Reduction of area, %.

The differences observed in the values of  $\sigma_f$  (fracture strength) can be due to a reduction in plasticity. The API-X80 steel suffered a significantly greater drop in reduction in area in solution than the API-X70 steel, this may indicate a presence of hydrogen, since the Reduction of area drop was smaller than that observed when tested in air and the fracture strength was higher, indicating some embrittlement.

The degree of (SCC) susceptibility, as measured in the SSRT is expressed using a relative ductility parameter. An analysis of the above parameter reveals that the effective ductility of the API-X70 and API-X80 steels was, in fact, significantly reduced exhibiting ratios (of

results in air/results in solution) of much less than one [30], indicating susceptibility to HE. Despite this fact, secondary cracks were not revealed in the fractographic analysis.

The reduction in ductility observed, can be attributed in this case, to a loss in the intrinsic toughness of the steels when submitted to an aggressive environment, Figure 10, independent of the presence of any secondary cracks. Such cracks, would normally be associated with the recombination of hydrogen atoms, previously in solid solution, to form hydrogen molecules at microscopic interfaces. This form of recombination often occurs at non-metallic inclusions. The observed loss in strength/ductility was manifested at relatively high stress levels, a condition in which even quite low concentrations of hydrogen can provoke a loss in toughness.

In the case of the tests carried out according to the NACE TM 0177/96 – Method A (Standard Tensile Test) norm [6], test piece rupture occurred for neither the API-X70 nor the API-X80 Grades after 720h of exposure at 80 percent of the YS, Figure 11, despite H<sub>2</sub>S levels for the standard NACE solution, orders of magnitude higher than those present in the thiosulphate-based solution used in the SSRT. The NACE test samples were also examined metallographically, and in this case, no cracks were observed to have formed as a result of the test.

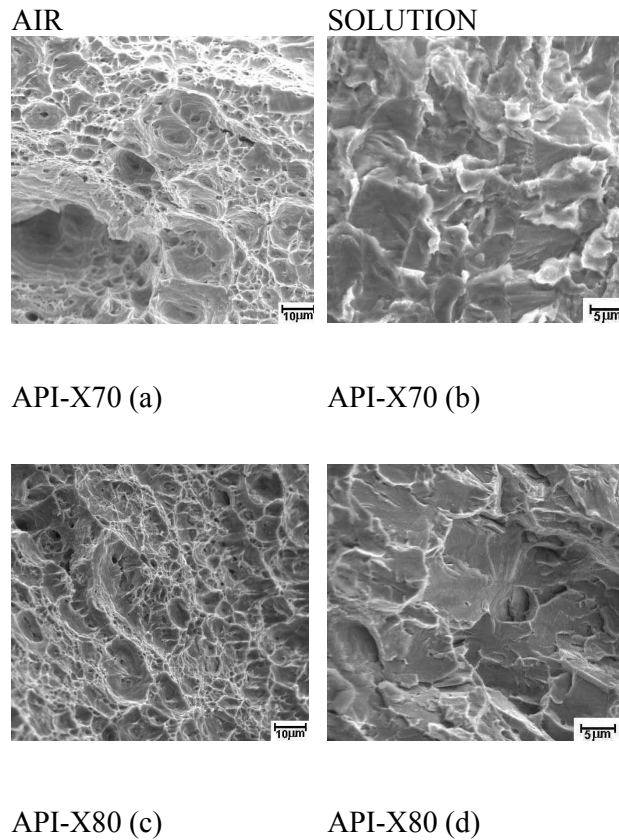


Figure 10 – SEM analysis of API-X70 and X80 test pieces tested in air (a,c) and in the Thiosulphate-based Solution (b,d).

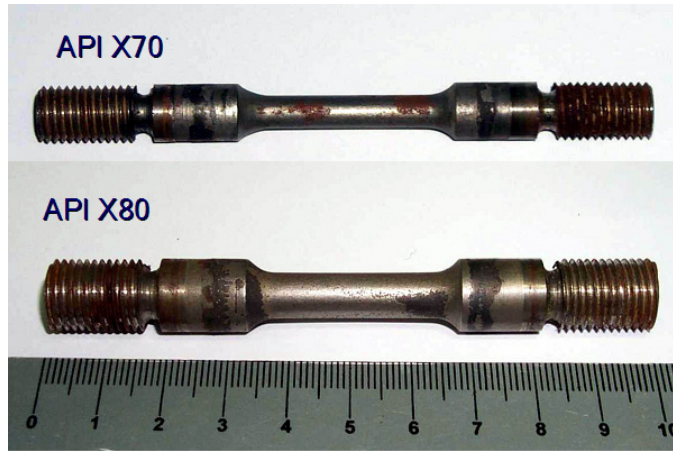


Figure 11- Aspect of test pieces subjected to constant loading at 80 percent of  $\sigma_y$ , after 720 hours, where fracture did not occur for these samples.

The results for both steels can be interpreted as being due to the elevated resistance of the microstructures to the nucleation of defects resulting from hydrogen recombination-induced damage. The apparent absence of the embrittlement effect, previously detected in the SSRT, could be due to lower imposed stress levels and the static nature of the NACE test loading as compared with the dynamic, high stress regime SSRT.

### Welded Joints

The same methodology was applied to longitudinal welds of alloy G (table 1). The carbon equivalent measures the hardenability, and it is considered that alloys with higher  $P_{cm}$  values have higher susceptibility to hydrogen cracking [31], although this behaviour can be attributed to the alloy carbon content, there are other alloying elements that can contribute to the hardenability. Therefore different chemical compositions, even with lower carbon content, can have the same hardenability as others of higher carbon content [32].

The alloys studied have similar  $P_{cm}$  not only for the base metal but also for the weld metal. Therefore both base metals would be expected to form heat affected zones of similar hardness. This, however, was not observed, the HAZ (heat affected zone) of the X80 steel exhibited a hardness 15 percent higher than the X70 steel. This could have been due to the presence of a higher level of Cr in solution in the case of the X80 steel. The yield strength is also a parameter, used to indicate the tendency to SSC susceptibility, generally being limited to 690MPa [33]. In this case none of the welded joints (Table V) should be susceptible to failure.

Table VIII - Yield Strength of the steels studied.

Region	Yield Strength (MPa)	
	API-X70	API-X80
Plate	482	550
Base Metal (tube)	433	622
Welded Joint	540	659

The degree of (SCC) susceptibility, as measured in the SSRT, is expressed using a relative ductility parameter. In this case, although both values are less than 1.0, and both welded joints showed some degree of susceptibility, the X70 presented more susceptibility (0.05) than the X80 (0.1).

All samples failed when tested in air and in solution and metallographic analysis identified that the rupture occurred in the base metal for both alloys. The X70 in solution showed cracks perpendicular to the applied tension, which are characteristic of SCC.

However, it should be pointed out that these samples were taken parallel to the rolling direction, which is the direction characteristic of HE cracks [33]. In this case the cracks were evident when the X70 was tested in the thiosulphate solution, indicating SSC susceptibility.

Furthermore, permeation tests [7] demonstrated a difference in hydrogen permeation current for the two steels. The steady state current measured for API-X70 steel was higher than that obtained for API-X80, for the same sample thickness and testing conditions. The results for the welded joint of API-X70, showed that the influence of the microstructure type in the SSRT, confirmed the general tendency that the ferritic-pearlitic base metal microstructures are more sensitive to SCC than the HAZ or the weld metal, even when these have higher hardness, but still below the maximum of 248HV.

The strength level of 690MPa is also generally considered a limiting value. Even though the welded joints in this study presented yield strengths below this value, both alloys exhibited cracks, but the alloy with the banded microstructure was more susceptible.

It has been shown that the nucleation and growth of SCC cracks in steels of medium and high strength occurs perpendicular to the direction of the applied tension [34]. In the present case, the study of longitudinal SAW joints, the sampling only allowed the applied tension to be perpendicular to the rolling direction. This arrangement led to the possibility of cracks appearing parallel to the rolling direction, and consequently perpendicular to the applied tension stress, raising the question of which is the controlling factor. One possible explanation, since SCC is dependent on the interaction of several parameters, such as environment, microstructure and applied stress, could be the higher hydrogen permeability of the ferritic-pearlitic microstructure, compared to the granular bainitic or ferrite with MA. In the present case the classification of SCC cracks and HIC is not applicable.

The NACE TM 0177/96- Method A test was undertaken at 80 and 100 percent of the yield strength of the base metal of each welded joint. None of the joints failed at 80 percent of YS after 720 hours, and according to this standard they were considered approved. At 100 percent all samples failed except one, however at different times, though all of them at less than 720 hours. Figure 3 shows the fracture for the shorter times, of failure. It should be observed that for the API-X70, the failure occurred in the weld metal while for the API-X80 the failure occurred in the base metal. Considering that the strength of the welded joint in both cases was higher than that of the base metal (body pipe), as shown in Table 5, the effective strength applied to the whole welded joint, including the weld metal and heat affected zone was less than 80 percent or 100 percent, therefore being a very conservative methodology. Considering the API-X70 from a microstructure and hardness point of view, it can be seen that the weld metal was the hardest region at 229HV<sub>5</sub>, although below the maximum of 248HV<sub>5</sub>. The ferritic microstructure of the weld metal is not usually considered susceptible to SCC, but in this case the applied tension may have exceeded 100 percent of the YS.

In considering the parameters utilized to determine the susceptibility to SCC (loss of ductility, microstructure, hardness, Pcm and yield strength) and applying these to the SAW welded joint of the steels studied, it was observed that at least one of the regions of the welded joints can be considered as susceptible to SCC and HE from the results of SSRT and NACE tests. The effect of welded joint strength is a result of a complex interaction of base metal, heat affected zone and weld metal. The most important characteristics for the welded joint of the API-X70 were the base metal microstructure and the weld metal Pcm. In the case of API-X80 the weld metal Pcm and the welded joint YS were the most relevant factors. Nonetheless when tested by SSRT, failure occurred in the base metal of both alloys and for NACE tests at 100 percent of YS the failure occurred in the WM for the API-X70 and at the BM for the API-X80. As mentioned previously the SSRT mechanism is associated with the

plastic straining imposed while in the NACE test is related to hydrogen accumulation suggesting that for pipeline steels the SSRT seem to give better behaviour prediction.

### **Induction Hot Bending**

During pipe bending, the main dimensional changes are extrados wall thickness decrease, intrados increase, changes in pipe diameter and ovalization. Wall thickness measurements were performed using an ultrasonic thickness gage. These measurements were made in the intrados, extrados and tangent end. Pipe diameter and ovalization measurements also were performed. The pipe diameter decreased by only 0,1 percent.

According Williams [35], the decrease is attributed to thermal expansion and contraction effects as the pipe passes through the induction coil.

The ovalization was relatively small (only 0,5%), calculated as the difference between the largest and smallest external diameters divided by nominal diameter. The slight amount of ovalization can be attributed to the relatively small diameter/wall thickness relation. The intrados wall thickness increase was 9,8 percent and extrados decrease was 8,4 percent. The pipe for hot bending process should take into account these dimensional changes.

During induction hot bending the maximum temperature to which the steel is heated usually exceeds the upper critical temperature for 1 to 2 minutes; thus the microstructure of the steel is transformed to austenite. Immediately after passing through the induction coil, quenching by water follows. Different points, around the pipe circumference pass through the induction coil at different speeds [35], depending on their distance from the bend axis. It should be noted that the outer radius would be under the induction coil for a shorter time than would be the inner radius.

A significant microstructural change was observed across the wall thickness. The outside surface has a more acicular microstructure due the higher cooling rate caused by outside water quenching, resulting in high hardness values. When compared with other bend areas, the intrados had higher austenitic grain growth because this region had a longer exposition time at bending temperature. The transition zone microstructures are very similar to the original (tangent ends). However, due to the start and stop bending procedures, a greater variety of grain sizes was observed (Figure 12), the hardness of these regions are shown in Figure 13, compared with the tangent end.

In a bent pipe, normally, there are significant differences in mechanical properties from tangent ends to bent region and between different locations around the pipe circumference. The temperature associated with the 100J absorbed energy level in the impact tests decreased after bending. The tangent end transition temperature is about 30°C above the intrados and about 40°C above the extrados transition temperatures.

The behaviour of the transition zones is very similar to the original pipe which also has higher transition temperatures than the bent region.

In general, toughness improved after induction hot bending. One reason for this improvement is the presence of alloying elements such as niobium, vanadium and titanium that precipitate as carbides and nitrides, during induction heating. The resulting fine precipitates suppress austenite grain growth.

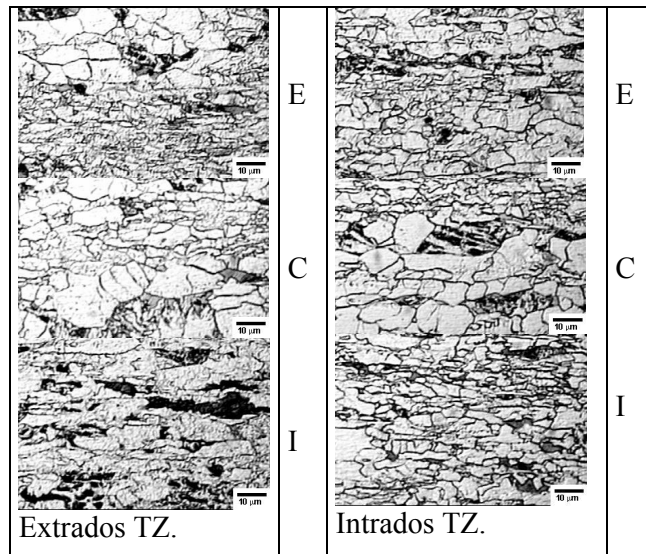


Figure 12 - Transition Zone Microstructures. Optical Microscopy, for the E=extrados, I=intrados, C=central regions, Magnification: 500X. Etch: 2% Nital.

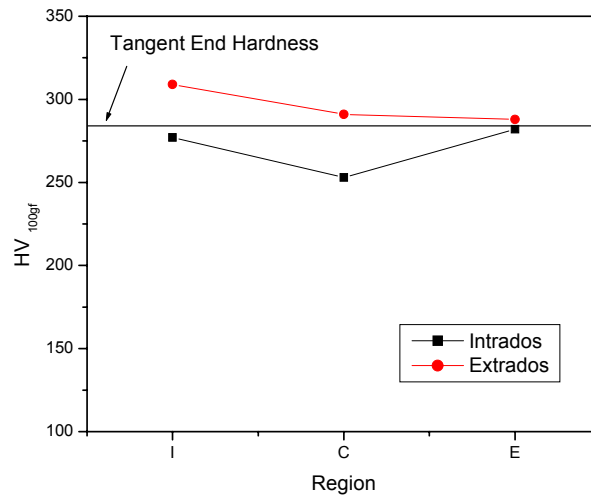


Figure 13 - Vickers hardness for the transition zone region

Kondo et al [36] showed that although the austenite grain size of the niobium bearing steel increases with an increase in heating temperature, because an increase in heating temperature promotes solution of Nb (C, N) in the austenite phase, it is clear that the grain size is much smaller than that of the niobium free steel.

A fine austenite grain leads to a fine microstructure after quenching and hence good toughness. Vanadium and titanium precipitates have a similar effect however with different dissolution temperatures. TiN, for example, is stable at high temperatures and this is very effective in suppressing austenite grain growth. Furthermore the hot bending process promoted small ferrite grain formation and reduced work hardening, benefiting toughness [37,38].

In spite of high toughness, the low carbon niobium steels have low hardenability (low carbon equivalent) and for this reason, it is necessary to add other alloying elements to meet the required strength. The yield strength measured in the bend region (extrados, intrados and neutral axis) was appreciably lower than that of the original pipe and also lower than the specified minimum yield strength (SMYS). The yield strength reduction can be explained by the low carbon equivalent (CE) level. For straight pipes the low CE assures good weldability

but, on the other hand, does not provide the necessary hardenability to assure the high strength in bends made by quenching. For this reason the pipe must have a CE content suitable for the hot bending process.

Previous work [39] showed an optimum CE value of 0,48 percent for the X80 grade. This value assures good strength after bending. The steel in this study has a CE of only 0,42 percent. After Kondo [40] the cooling rate is also an important parameter and strongly depends on wall thickness. Therefore the, application of a method with cooling from both inside and outside for induction bending in high strength steel pipe (and/or heavy wall thickness) increases the cooling rate and is effective in reducing the critical CE. Thus high strength can be achieved with low CE steel by cooling from both sides. Another way to improve yield strength is perform a separate heat treatment after bending.

In the bending process, the bent region and tangent end weld seams have significant differences. A tangent end weld seam is in the as welded condition while the bent region is quenched. If a tempering heat treatment is applied, the bent region will be quenched and tempered and the tangent ends only tempered. Therefore, it is necessary to design alloying element additions to obtain sufficient properties for both the bent region and the tangent ends under the different thermal conditions.

Charpy impact test showed that the weld metal has the highest transition temperature and the heat affected zone (HAZ) has the lower. These results are in agreement with previous work [3] that attribute high HAZ toughness to the microstructures transformations induced by the welding thermal cycle where the size, shape and distribution of MA constituent is the main cause of high HAZ toughness.

The Vickers microhardness values of the base metal, weld metal and HAZ are very similar in the range 295-278 HV<sub>100</sub>. However, it is noted that the HAZ has the lowest average hardness (278 HV<sub>100</sub>) and the weld metal the highest. Similar results were found for a 30" pipe with 0,625" wall thickness produced by the same production route as the pipe studied here [40].

As well as the base metal, the weld metal and HAZ also present a significant change in mechanical properties after hot bending. The induction hot bending process, results in removal of the HAZ in the bending section, and appreciable homogenisation and grain refinement of the weld metal [35]. It results in a HAZ and weld metal toughness improvement, decreasing the transition temperature. The lower HAZ hardness does not impair the weld seam strength. For all regions evaluated, the weld seam strength is higher, at approximately 750MPa, than the base metal strength, at approximately 705 MPa. Although HAZ softening has been observed in high strength steel welded using the submerged arc welding process (tandem technique) [35], the HAZ softening did not affect the tensile strength values [40,41].

In order to improve the yield strength after induction hot bending, a tempering heat treatment was applied, heating up to 300 °C with a free heating rate, then heating between 300 and 500 °C with a heating rate of 100°/h, followed by soaking at a temperature of 500 °C for 1 hour and cooling in air. The heat treatment was evaluated only in the intrados and extrados regions. Although the heat treatment applied did not re-establish the original X80 yield strength, it did, however, increase it to above the minimum value required by the API 5L standard.

The yield strength improvement is related to precipitation hardening caused by the presence of alloying elements. These elements are in solid solution at the bending temperature and remain so due to the high cooling rate promoted by water quenching. During the tempering heat treatment, precipitation occurs, resulting in the yield strength increase.

## Summary

According to the results obtained in the first part of this research program, for the Nb-Cr and NbCrMo steels and considering that the API 5L standard specifies a toughness criterion of 68J at 0°C in the transverse direction, the alloys of this study showed, an average energy at – 20°C of 200 J for the plate, 150 J for the body pipe and 190 J for the HAZ.

These results indicate that the alloys for both systems had satisfactory performance, meeting the relevant API 5L specifications. Furthermore, the welding procedure used in the study, involving the utilization of several electrode types, with a range of mechanical properties, produced a joint which was adequate to meet the API 1104 standard, and despite the high strength of the (Ferrite + Bainite + MA) base metal, no significant loss in toughness was observed for the heat affected zone, and the preheating and interpass temperatures used permitted the avoidance of cold cracking. The welding parameters used resulted in microstructures throughout the joint, which exhibited satisfactory toughness levels.

Regarding the environmentally induced cracking of both steels, the deterioration mechanism observed under static load in the NACE solution and under SSRT in sodium thiosulphate solution presented different characteristics. In the NACE solution the most important determining factor was the hydrogen accumulation in the steel. In sodium thiosulphate solution the predominant effect of hydrogen would be the same intrinsic toughness reduction of the material enhanced by the plastic straining imposed during SSRT. The results for both steels can be interpreted as being due to the elevated resistance of the microstructures of these materials to the nucleation of defects resulting from hydrogen recombination-induced damage.

The loss in ductility of the API-X70 and API-X80 steels, which was observed to result from SSRT in H<sub>2</sub>S-generating thiosulphate-based solution, indicates potential hydrogen embrittlement susceptibility. Both of the steels investigated exhibited good levels of SCC resistance as measured by the standard NACE test, showing no loss of strength under the specified conditions. In neither of the tests were secondary cracks detected after loading in H<sub>2</sub>S-containing media. This is probably due to the very low non-metallic inclusion levels in the materials studied.

The results obtained from the first part of this study lead to the conclusion that an API-X80 pipe, produced without accelerated cooling, meets all requirements of API 5L Standard for X80 grade. However the pipe is suitable only for use where bending operations are not required. For field welding, special attention should be paid to the training of welders because the procedure and the electrode types are not those traditionally used.

The results for the second part of this research program, ongoing at the present date, concerning hot induction bending, lead to the conclusion that, the extrados wall thinning is about 8 percent, therefore it should be taken into account during pipe wall thickness design.

The outside water-cooling, after the pipe has passed through the heating coil, results in a microstructure variation through the wall thickness, where the hardness values can vary from 260 HV (inner surface) to 350 HV (outer surface). These hardness values, however, are in agreement with the pipe specifications. After bending, there was a significant toughness improvement in the bent region, which was related to new small ferrite grain formation and work hardening reduction. Furthermore, the alloying elements such as niobium, vanadium and titanium precipitate as carbides and nitrides, during induction heating, resulting in fine precipitates that suppress austenite grain growth. The X80 weld metal chemical composition was suitable for the hot bending process, since this process improved the weld metal, HAZ and base metal toughness. The HAZ at the tangent end, transition zone and bend region, exhibited the lowest transition temperature and hardness, also the weld seam tensile strength was higher than that of the base metal, for all regions evaluated.

The hot bending process reduces the bend region (extrados, intrados and neutral axis) yield strength produced during the controlled rolling process (without accelerating cooling). This is associated with the low CE level, which does not provide the necessary hardenability to assure adequate strength in the quench process. There has been a suggestion that the application of a cooling water from both inside and outside could minimize the yield strength reduction.

By tempering, significant yield strength improvement of the extrados and intrados was achieved, increasing this value to above the minimum required by the API 5L standard. This improvement is related to precipitation hardening mechanism caused by the presence of microalloying elements. The precipitation effects on yield strength depends on particle size and their distribution in the matrix as well as on heat treatment parameters.

### **Acknowledgments**

Three of the authors, Ivani de S. Bott, Luís Felipe G. de Souza and Paulo R. Rios, wish to acknowledge the financial support of FINEP and PETROBRAS and the technical support of USIMINAS, CONFAB and CENPES-PETROBRAS for this study. The authors are also grateful to CNPq and FAPERJ for their financial support.

### **References**

1. Gray, J. M.; Fazakerley, W. J.: Annual Conference of Metallurgists, 1998, 37, pp.1-31.
2. Petrobras 2015 Strategic Plan. Available in: <<http://www.petrobras.com.br>>. Access date: December 06, 2005.
3. Bott, I. de S., Souza, L.F.G de, Teixeira, J.C.G., Rios, P. R., High-Strength Steel Development for Pipelines: A Brazilian Perspective, Metallurgical and Materials Transactions, 2005, 36A, pp.443-454
4. API Specification 5L, Forty-Second Edition, July 2000.
5. API Standard 1104, Nineteenth Edition, September 1999
6. NACE TM0177/96 Method Nace International, December 1996 Laboratory testing of metals for resistance to specific forms of environmental cracking in H<sub>2</sub>S environments. NACE Standard TM0177/96. Standard Test Method. Texas.
7. Lima, K. R. de S., Bott, I. de S., Ponciano, J. A. G., International Conference on Offshore Mechanics and Arctic Engineering (OMAE 2005), CDROM
8. Lima, K. R. S., 2002, SCC Behavior of API steels, MSc Thesis (in Portuguese), PUC-Rio Dept. of Materials Science and Metallurgy.
9. Batista, G. Z., Hippert Jr, E., Naschpitz, L., Bott, I.de Souza, Induction Hot Bending and Heat Treatment of 20 Inch API 5L X80 Pipe, IPC06-10089, IPC 2006, to be published
10. Specification for Line Pipe, API Specification 5L. American Petroleum Institute, March. 2004.
11. Standard Test Methods and Definitions for Mechanical Testing of Steel Products. ASTM A 370. American Society for Testing and Materials. 2003.

12. Sage, A. M.: The Metals Society, 1981, pp. 39-50.
13. Dixon, B; Hakansson, K. Welding Journal, 1995, 74, pp. 122s
14. Dhua, S.K.; Mukerjee, D.; Sarma, D.S.: ISIJ International, 2002, vol. 42, n°. 3, pp.290-298.
15. Nagae, M.; Endo, S.; Mifune, N.; Uchitomi, N.; Hirano: NKK Review, 1992, n°. 66, pp.17-24.
16. Hart P. H.: Canmet, Ed. J.D. Boyd and C. S. Champion, 1985, pp. 435-454.
17. Kozasu, I.: Proceedings of an International Symposium on Welding Metallurgy of Structural Steels, Ed. J.Y. Koo, TMS, 1987, pp. 63-77.
18. Li, Y.; Crowther, D.N.; M.; Green, J. W.; Mitchell, P.S.; Baker, T. N.: ISIJ International, 2001, vol. 41 n°. 1, pp.46.
19. Thompson, S.W.; Krauss, G.: Mechanical Working and Steel Processing Proceedings, 1989, pp. 467-481.
20. Thaulow, C.; Paauw, A. J.; Guttormsen, K.: Welding Journal, 1987, vol.59 n°. 9, pp. 266s-279s.
21. Davis, C. L.; King, J. E.: Materials Science and Technology, 1993, vol. 9, pp.8-15.
22. Matsuda, F.; Fukada, Y.; Okada, H.; Shiga, C.; Ikeuchi, K.; Horii, Y.; Shiwaka, T.; Suzuki, S.: Welding in the World, 1996, vol. 37 n°. 3, pp. 134-154.
23. Jorge, J.C.F.; Souza, L.F.G.; Rebello, J.M.A.: Revue de La Soudure, 1996, vol.3, pp. 42-50.
24. WidgerY, D.J. Welding high strength pipelines from laboratory to Field, Svetsaren n°2, p.p.22-25.
25. Hillenbrand, H, Niederhoff, K. A., Hauck, G., Perteneder, E., Wellnitz,G. Procedures, Considerations for Welding X-80 Linepipe Established. Oil and Gas Journal, Sept 15, 1997, p.p.47-56.
26. Mee, Vincent Van der, Neessen, Fred. Development of High Strength Steel Consumables From Project to Product. 2nd International Symposium on High Strength Steel, ECSC European Research Project PRESS, 23-24 April 2002, Verdal Norway.
27. Patel, J. K., January 2001, A brief report on the influencing factors on SCC in buried pipelines, Germany: Niobium Products Company GmbH (NPC).
28. Psaila-Dombrowski, M. J., Van Der Sluys, W. A., Miglin, B. P., 1997, Investigation of pipeline stress corrosion cracking under controlled chemistry conditions. Gas Research Institute, GRI Contract No 5093-260-2642, Chicago, IL
29. National Energy Board, MH-2-95, November, 1996, Report of the Public Inquiry, Stress corrosion cracking on Canadian oil and gas pipelines, Calgary, Alberta, Canada, pp. 1-158.

30. Small, A. L. L. T, 1996, Study of SCC and HE in Martensitic and Austenite-Ferrite Stainless Steels Using SSRT, MSc Thesis (in Portuguese) COPPE/UFRJ, Rio de Janeiro.
31. Omweg G. M., Frankel, G. S., Bruce W. A., Ramirez J. E., Koch G., Welding Research, (2003) pp 136s
32. Martins, F. A., Ponciano, J.A., Bott I. de S., Saw Welded Joints of Two API Steels Subject to SCC Laboratory Testing, THERMEC 2006, to be published.
33. NACE MR0175 Materials Equipment Standard – Sulphide Stress Cracking Resistant Metallic Materials for Oilfield Equipment, Houston, Texas.
34. Kane R.D., International Metals Reviews, vol30 (1985), No. 6, p.291
35. Williams, D. N. Investigation of the Properties of Induction Hot Bends. Battelle Columbus Division. Seventh Symposium on Line Pipe Research. PRCI. October, 1986.
36. Kondo, J. et al. The State of The Art of High Strength Induction Bent Pipe. NKK Corporation. Eighth Symposium on Line Pipe Research. PRCI. September 1993.
37. Hulka, K. Metallurgical Concept and Full-Scale Testing of High Toughness, H<sub>2</sub>S Resistant 0.03%C-0.10%Nb Steel. Niobium Technical Report. CBMM.
38. Sage, A. M. Physical Metallurgy of High-Strength, Low-Alloy Line-Pipe and Pipe-Fitting Steels. The Metals Society, Vol. 10, p. 224-233, June 1983. London.
39. Behrens, D.; Hillenbrand, H. G. And Speth, W. Induction Bends in Grade GRS 550TM/V (X80). Europipe. 1994.
40. Batista, G. Z. SOUZA, L.F. G., BOTT. Ivani de S., Submerged Arc Welding Weldability of API-X80 Steel. 58° ABM Annual Congress. July 21-24, 2003. Rio de Janeiro. (In Portuguese).
41. Nagae, M. et al. Development of X100 UOE Line Pipe, NKK Review, n. 66, p. 17-24. 1992.